Jurnal Teknologi

Full Paper

DEVELOPMENT OF HIGH-PERFORMANCE GEOPOLYMER PASTE UTILIZING LOCALLY NANO-METAKAOLIN

Riyam Imad Jaddan[a,b]*, Hussein Alaa Jaber[a]

[a]Department of Materials Engineering, University of Technology, Alsinaa Street 52, 10066Baghdad, Iraq
[b]Department of Materials Engineering, College of Engineering, University of Al-Qadisiyah, 58001, Al Diwaniyah, Iraq

Article history
Received
24 December 2024
Received in revised form
23 March 2025
Accepted
25 March 2025
Published Online
23 December 2025

*Corresponding author
mae.22.037@grad.uotechnology.edu.iq

Graphical abstract

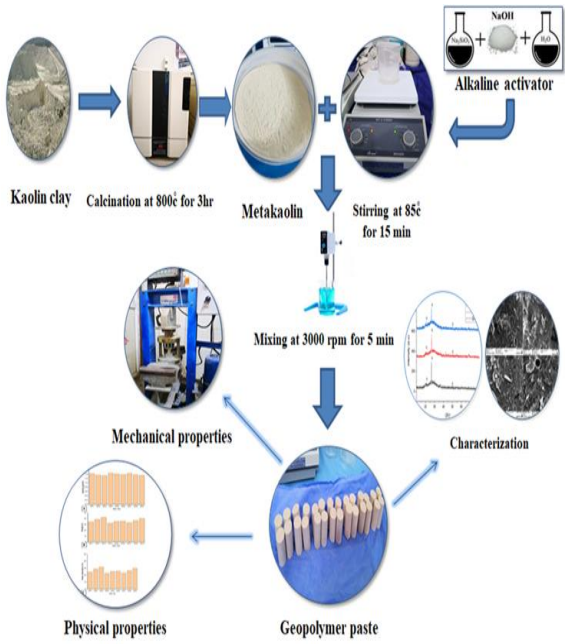

Abstract

Geopolymers have attracted the attention of researchers due to their exceptional performance and potential to replace Portland cement-based materials, attributed to their low energy consumption and reduced global warming potential This work goal is to develop a high performance geopolymer paste (GP) and investigate the effect of varying water to metakaolin ratio dosages, as well as the impact of different silica to alumina ratio on it. Nine mixes were cast and curing for 28 days at ambient temperature. Compressive tests were performed at 7 and 28 days to evaluate mechanical qualities. Other parameters, including bulk density, porosity, water absorption, chemical compositions (analyzed by XRD), and microstructural features (analyzed by SEM), were also measured. Results showed that the optimal silica to alumina ratio and water to metakaolin ratio is 1.825 and 0.54 respectively that generate the highest compressive strength (88.4 Mpa) with lower water absorption (22.7 %), porosity (32.3%), and density (1.45%).

Keywords: Geopolymer, metakaolin, SEM, compressive strength, water absorption

1.0 INTRODUCTION

The projected increase in global population, expected to surpass 9.8 billion by 2050, drives the demand for sustainable construction, urbanization, industrialization, and infrastructure development. This, in turn, intensifies the need for construction materials on a massive scale. Over the past 50 years, the output of concrete has surpassed that of other building materials due to the widespread recognition of ordinary Portland cement (OPC) as a crucial component, and the rise in per capita consumption has surpassed the rate of population growth [1]. The production of (OPC) depletes significant amounts of natural resources and releases enormous amount of greenhouse gases, contributing to global warming [2-6]. Annually, OPC manufacturing is responsible for approximately 1.5 billion tons of greenhouse gas

emissions, accounting for 5–8% of global emissions [7]. Reducing the carbon footprint through efficient remedial actions is essential for the sustainable development of the cement sector. Consequently, research efforts have focused on exploring alternative sustainable materials. Alkali-activated materials (AAMs) have drawn a lot of interest in recent decades as alternative sustainable materials due to their outstanding mechanical characteristics and environmental pollution mitigation. The French investigator Davidovits at 1970's developed the first calcined kaolin materials with low calcium content for producing AAMs, the term "geopolymer" was used to emphasize the inorganic character of the related binder and its structural resemblance to polymers [8, 9].

Later Joseph Davidovits claims that because geopolymers are not a substitute for calcium hydrate, they cannot be classified as a subgroup of AAMs. The chemical processes that take place in geopolymers are polymerization reactions rather than hydration or gelation events. The word "geopolymer" is created when an alkaline activator reacts with an aluminosilicate material, while AAM encompasses a wider range of alkali-activated materials, including fly ash and alkali-activated slag, which may or may not exhibit actual polymerization, and they differ in their chemical compositions, nanostructures, and characteristics. Because of this, there are notable differences between AAMs and geopolymers in terms of durability, molecular structure, and reaction chemistry [10, 11].

Generally, geopolymers are aluminosilicate inorganic materials synthesized through a polycondensation reaction known as geopolymerization process [12, 13]. This process involves an inhomogeneous chemical reaction of either alkaline or acidic solutions and precursor materials containing alumino-silicate [14], that encompasses various materials such as fly ash [5, 15-17], slag [13], red mud [18, 19], metakaolin [20-22], corncob ash [23], rice husk ash and bagasse ash [24]. the chemical formula for geopolymer expressed by Davidovits is as follows: $M_n[-(SiO_2)_z\text{-}AlO_2]_n.wH_2O$, where M: represent the metal cation (Ca^{2+},Na^+,K^+), n: degree of geopolymerization, z: Si/Al molar ratio and *w*: water molecules quantity [25, 26]. Numerous researchers have sought to establish the optimal M/Al ratio for synthesizing MKGs, with a ratio of 1 being recommended [27, 28], A noteworthy observation was reported for the expression of geopolymer composition as $1Na_2O.1Al_2O_3.{}_nSiO_2.wH_2O$ [29-31]. To date, numerous research has been documented that concentrated on a wide range of parameters that influence the geopolymer behavior and performance, such as curing methods [32], alkaline type , solution molarity [33], raw material [1, 34]. As far as the authors are aware there is limiting research on local metakaolin as an aluminosilicate source and the impact of the processing parameter on the geopolymer performance according on the aforementioned chemical formula expression.

The present study aim to identify high performance geopolymer paste mixtures while rigorously examining the influence of the Si/Al molar ratio and the water-to-metakaolin ratio on the physical properties and compressive strength of locally produced metakaolin geopolymer. Also the microstructure have been investigated.

2.0 METHODOLOGY

2.1 Materials

2.1.1 Raw Material

Nano Iraqi kaolin, with chemical composition of $Al_2Si_2O_5(OH)_4$, from the local area "Al-Mishraq (Mosul, Iraq)" was utilized as an aluminosilicate material for the geopolymer paste preparation. Calcination process was made at 800° for 3hr in an atmosphere with a heating rate 5 ℃/min to convert the crystalline kaolin structure into amorphous Metakaolin [35], then preserved it in glass containers to prevent the humidity exposure. The metakaolin produced in this study will be referred to as (nano-MK-800). nano-MK-800 X-Ray Fluorescence (XRF), Particle Size Analysis (PSA), X-Ray Diffraction (XRD), and Fourier transform infrared spectroscopy (FT-IR) analysis results are presented in Table1, Figure 1, Figure 2 and Figure 3 respectively.

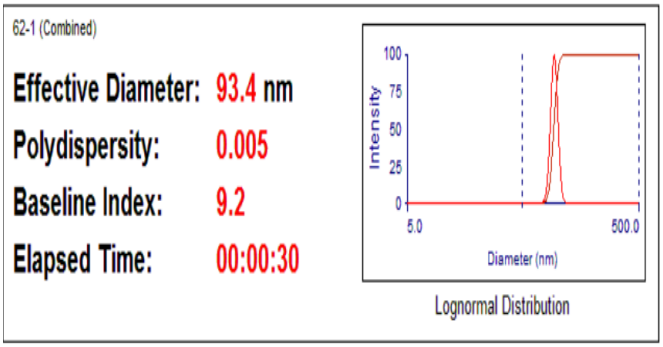

Figure 1 PSA of Nano-MK-800

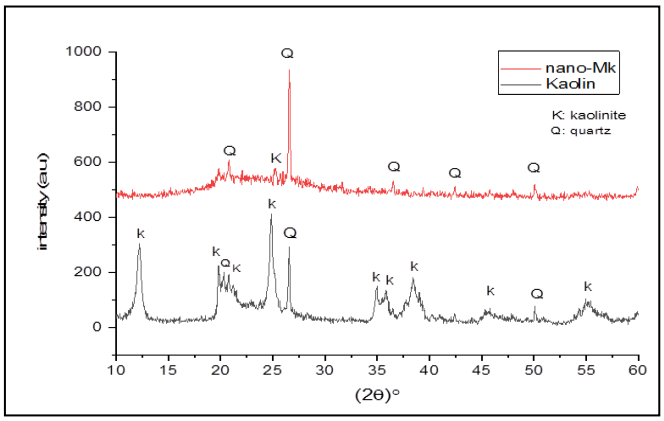

Figure 2 XRD patterns of kaolin and nano-MK-800

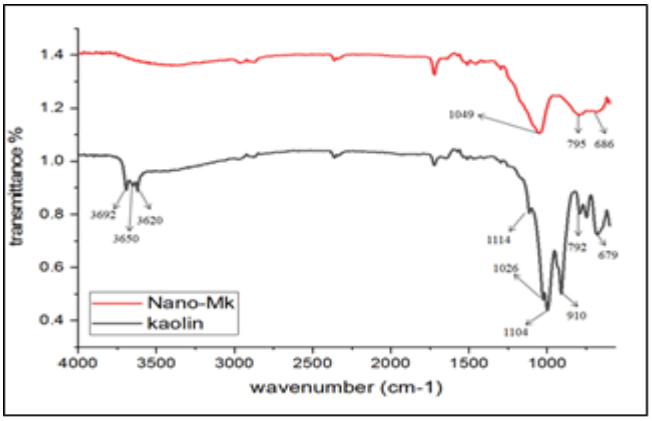

Figure 3 FT-IR spectrum of kaolin and Nano-MK-800

Table 1 nano-MK-800 Chemical composition

Chemical composition	percentage %
K_2O	0.527
Na_2O	0.087
CaO	0.619
Al_2O_3	31.51
MgO	0.11
SiO_2	45.81
Fe_2O_3	1.824
TiO_2	2.03
SO_3	0.275

Figure 1 delineates the particle size distribution of MK-800 as characterized by the Particle Size Analyzer (PSA). The assessment elucidates that MK-800 exhibits a predominant particle size of 93.4 nm, underscoring its ultrafine nature. This fine particle dimension engenders a substantial surface area, thereby augmenting the intrinsic reactivity of metakaolin within the geopolymerization process. The observed particle size dispersion is a pivotal determinant in modulating the rheological behavior, and mechanical fortification of the synthesized geopolymeric matrix.

While Figure 2 illustrated XRD findings for kaolin and metakaolin where the distinctive peaks were noted using standard patterns ICCD cod (00-033-1161) for quartz and ICCD cod (00-001-0527) for kaolinite. The profile of diffraction verifies the transformation of the kaolin to the amorphous metakaolin, and it also show a sharp peak corresponding of free SiO2 (quartz).

Figure 3 displays the infrared spectra of kaolin and Nano-MK-800. The characteristic bands of 3692, 3650 and 3620 cm^{-1} could be correspond to the OH vibrational mode of the hydroxyl group, While the band at 910 cm^{-1} is believed to reflect the deformation vibration of Al-OH, the other bands at 1004, 1026, and 1114 cm^{-1} are those of Si-O bonds [36]. The presence of band at 792 and 679 cm^{-1} is ascribed to the quartz vibrations [37]. This outcome is consistent with XRD patterns. The pattern of kaolin before and after calcination confirms the absence of O-H bands [36]. To sum up, the 800C° is sufficient to convert kaolin into metakaolin.

Table 1 presents the results of the XRF analysis of the Nano-MK-800. This confirms the XRD results regarding the presence of free quartz and aids in calculating its quantity. Due to its inertness, which renders it non-reactive during the synthesis process, quartz should be excluded from the composition calculation of the geopolymer.

2.1.2 *Alkali Alkaline Activator*

A combination of commercial Sodium Silicate (SS) and Sodium Hydroxide (SH) solutions was utilized as Alkali alkaline activator. The choice of these activators is due to the greater abundance and cost-effectiveness of sodium silicate/hydroxide solutions compared to potassium silicate/hydroxide solutions [38]. SS solution, sourced from DUBICHEM, comprising 54% water, 13.5% Na_2O and 32.5% SiO_2 with a specific gravity of 1.54, while SH obtained from KOUT-Kuwait with flakes likes shape, having a purity 98%. After the complete SH dissolved in the required amount of water and cool down to ambient temperature, SS was added and mixed under stirring at 600 rpm with heat treatment the solution at 85 ℃ for 20 min and leave the solution for 24 hr at ambient temperature to get ready to use as binding agent.

2.2 Geopolymer Paste Preparation

At first the Nano-Mk-800 added to the cooling alkaline activator solution then mixing with an overhead mixer at constant speed of about 3000 rpm to 5 min to achieve a homogeneous geopolymer cement paste. the second step is pouring the prepared paste in a plastic mold with a height 40mm and diameter of 20mm. To mitigate moisture loss and ensure proper curing conditions, the specimens were sealed using a polyethylene film, derived from a food-grade plastic bag. This film, with low permeability, served to prevent excessive water evaporation, ensuring optimal geopolymerization. cured for 24 hr at ambient temperature. Finally, the paste is demold and is kept at room temperature for the duration of the tests. This curing is preferred because it simplifies the usage of geopolymer in a variety of applications and lowers the expense of additional heating sources [39].

In this paper, nine different geopolymer mixes were trialed to finalise a geopolymer paste, The details of the mixes are shown in Table 2.

Table 2 show various geopolymer mixes to achieve the composition of geopolymer based nano-MK-800.

Mix No.	GP composition	Si/Al atomic ratio	W/MK ratio	Nano-MK-800 (kg/m³)	SS solution (g)	SH pellet (g)	W (g)
GP1	$Na_2O.Al_2O_3.3.6SiO_2.xH_2O$	1.8	0.54	400	367.7	35.216	18.5
GP2	$Na_2O.Al_2O_3.3.6SiO_2.xH_2O$	1.8	0.625	400	367.7	35.216	49.5
GP3	$Na_2O.Al_2O_3.3.6SiO_2.xH_2O$	1.8	0.7	400	367.7	35.216	80.5
GP4	$Na_2O.Al_2O_3.3.65SiO_2.xH_2O$	1.825	0.54	400	378.76	33.22	14
GP5	$Na_2O.Al_2O_3.3.65SiO_2.xH_2O$	1.825	0.625	400	378.76	33.22	45.25
GP6	$Na_2O.Al_2O_3.3.65SiO_2.xH_2O$	1.825	0.7	400	378.76	33.22	76.5
GP7	$Na_2O.Al_2O_3.3.7SiO_2.xH_2O$	1.85	0.54	400	390.55	31.27	9
GP8	$Na_2O.Al_2O_3.3.7SiO_2.xH_2O$	1.85	0.625	400	390.55	31.27	40
GP9	$Na_2O.Al_2O_3.3.7SiO_2.xH_2O$	1.85	0.7	400	390.55	31.27	70.5

2.3. Testing Methodology:

According to (ASTM C773-88) the compressive strength of 27 cylinder samples for each testing days (7,28), an average of three geopolymer paste samples, was taken using a universal material tester with a 50KN capacity and a loading rate of 3kn/ sec [40]. Archimedes method (ASTM C373-88) [41] was used to investigate the density (ρ), porosity (p%) and water absorption (WA%) of an average of the three samples from each geopolymer paste mix at 28 days. Following the fracture, the geopolymer paste was evaluated using scanning electron microscopy (SEM).

3.0 RESULTS AND DISCUSSION

3.1 Geopolymer paste Characterization

Figure 4 revealed XRD patterns result for 3 sample to show the effect of water, as shown from the diffractogram there is broad amorphous peak that extends at around (23–33) 2θ, which is the fingerprint of the geopolymeric reaction and this is an indication of the formation of (Sodium alumino silicate hydrate) NASH [42, 43]. It is important to highlight that the silica intensity in GP1 is higher than that in GP2 and GP3. The primary rationale for this difference is founded on the alkali activated solution viscosity. However, the increase in water content cause the viscosity to decrease, signalize that the inorganic polymeric substance had not fully dissolved the starting material, resulting in a geopolymer paste with a homogeneous mixture [44].

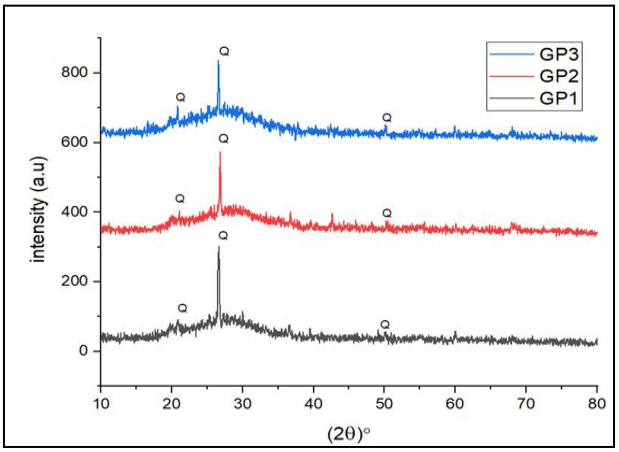

Figure 4 XRD patterns of prepared geopolymer paste

Figure 5 clarified the morphology of fracture surface observed by SEM. As it has been seen from the figure, there are a few spherical pores, some unreacted metakaolin and sparse micro-cracks. The presence of these micro-cracks were probably brought about by the selection of SEM samples from samples that had undergone compression testing or from the drying of geopolymer sample prior to scanning. Additionally, the observed pores may arise from air bubbles during the geopolymerization process, contributing to the overall porosity. In the tests, the unreacted metakaolin particles observed in the tests may be due to an elevated silica-to-alumina ratio, which contributes to the quantity of unreacted metakaolin [45, 46].

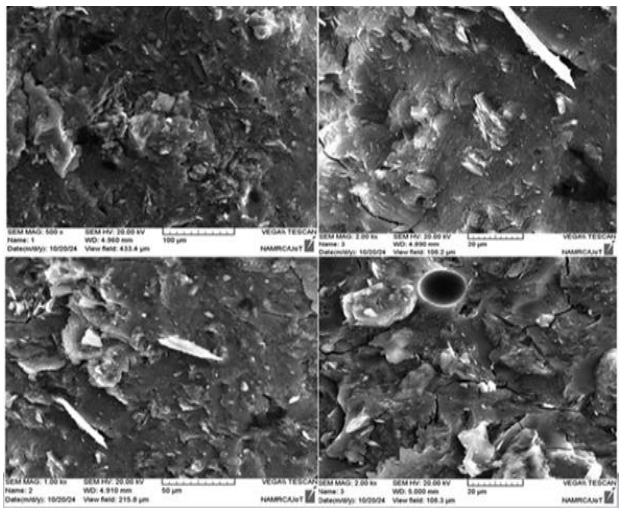

Figure 5 SEM morphology of prepared geopolymer paste GP4

3.2 Compression Strength

It predicted that the compression strength slightly increased with increasing in Si/Al ratio to 1.825 which consider the ideal value. Beyond this value, a discernible loss in strength was seen. The reason behind this, a high concentration of silicate species hinders the interaction between silicate and aluminate species. Because some silica remained unreacted in the resulting geopolymer gel as it can be seen in SEM image, the material lost strength as a result of the dissolution either not occurring at all or occurring in a reduced way [47]. On the other hand, lowering the ideal Si/Al ratio increases the aluminate concentration, leading to the formation the weaker Si-O-Al and Al-O-Al bonds, rather than the strong Si-O-Si bonds, causing the strength to decrease [48]. The impact of nanometakaolin is largely due to its small particle size, which provides a high surface area, thereby increasing the rate of dissolution in alkali media. This characteristic enhances its reactivity with the alkali activator.

The hydrolysis of dissolved Si^{4+} and Al^{3+} ions, along with the disintegration of solid particles, is facilitated by water, which acts as a medium for the geopolymerization process. It is evident that the compressive strength of geopolymer is significantly influenced by the water content. At lower water content of 0.54, a higher compressive strength is observed, whereas a higher water content of 0.7 experience a notable reduction in strength due to increased porosity within the geopolymer matrix. Furthermore, excess water accelerates the breakdown reactions, thereby diminishing strength, as the polymerization process is a condensation reaction [49]. Table 2 and figure 6 show the compression strength of prepared geopolymer mixes at 7 and 28 days.

Table 2 Compression Strength results of GP mixes at 7 and 28 days

Mix No.	7 day Compressive strength (Mpa)	28 day Compressive strength (Mpa)
GP1	70.6	85.6
GP2	62	78.1
GP3	51.5	60
GP4	74.7	88.4
GP5	72.6	76.9
GP6	62.1	69
GP7	67.6	84.9
GP8	65.6	74.5
GP9	45.9	72.3

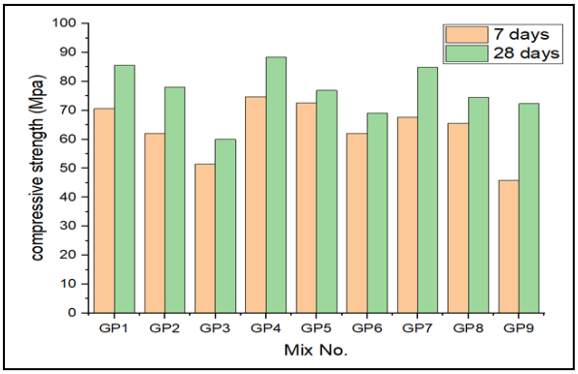

Figure 6 Compression strength of prepared geopolymer mixes

3.2 Physical Properties

Table 3 and Figure 7 depicts the inverse correlation between bulk density and water content, demonstrating that higher water content results in lower bulk density.

Table 3 Physical properties results of GP mixes at 28 days

Mix No.	density (g/cm^3)	Porosity %	Water absorption %
GP1	1.43	34.5	24.5
GP2	1.36	38.8	28.9
GP3	1.34	42.3	31.8
GP4	1.45	32.3	22.7
GP5	1.42	35.2	25.3
GP6	1.39	35.9	25.9
GP7	1.44	33.2	23.2
GP8	1.38	36.8	26.6
GP9	1.35	40.5	30

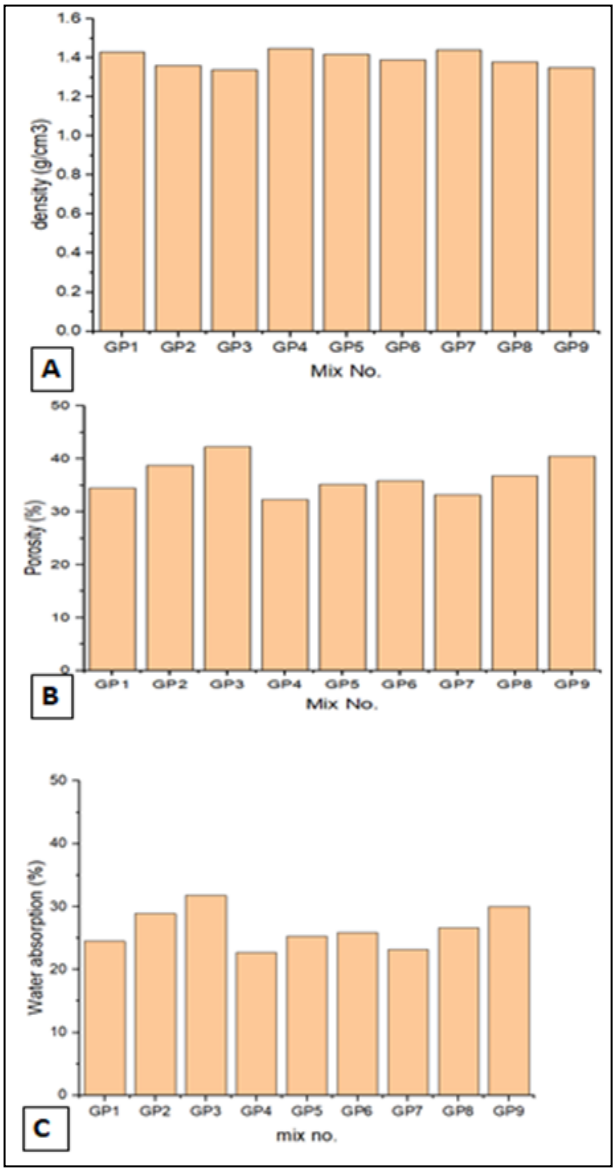

Figure 7 physical properties result for geopolymer mixes of A; density, B; porosity and C; water absorption

This reduction is primarily due to the evaporation of surplus water, which increases the pore volume within the hardened geopolymer matrix. The rise in porosity compromises the microstructural integrity by creating voids that interrupt the cohesion of the solid framework [50]. In contrast, porosity and water absorption increase proportionally with water content. This rise is mainly attributed to the presence of unreacted metakaolin particles and the formation of entrapped air voids, both of which enhance the overall permeability of the geopolymer matrix. An elevated water content dilutes the geopolymer precursor mixture, potentially hindering the complete dissolution of aluminosilicate precursors. This reduction in reaction efficiency results in a more porous and less compact structure [51]. The Si/Al molar ratio significantly influences porosity, water absorption, and bulk density. As the Si/Al ratio increases to 1.825, both porosity and water absorption show a slight decrease, which can be attributed to enhanced polymerization and the formation of a more stable and compact gel network. At this ratio, the geopolymerization process becomes more efficient, resulting in a denser matrix with improved mechanical properties. However, when the Si/Al ratio is raised further to 1.85, both porosity and water absorption begin to increase once again. This could be due to an excess of silicate species disrupting the optimal silicon-to-aluminum balance within the geopolymer network, potentially leading to incomplete reactions and the formation of microcracks or defects.

Bulk density exhibits a similar trend, increasing as the Si/Al ratio reaches 1.825, which indicates the formation of a more tightly packed and structurally cohesive geopolymer. This densification is likely the result of an accelerated geopolymerization reaction, which improves particle packing and minimizes pore spaces within the hardened matrix. However, beyond this ratio, the surplus silica may cause steric hindrance, preventing full reaction and leading to the development of additional voids, thereby lowering bulk density.

4.0 CONCLUSION

The effects of the Si/Al and W/MK ratios on the mechanical, physical, and microstructural properties of GP-based nanometakaolin were methodically analyzed. The following conclusions were drawn based on a rigorous examination of experimental data: Proper management of water and silica content is essential to produce geopolymers with a compressive strength of approximately 88 MPa. The highest compressive strength is achieved when the Si/Al ratio is 1.825, with a water-to-MK ratio of 0.54. An increase in the Si/Al ratio initially enhances compressive strength and density but results in a decline beyond a certain threshold. Conversely, porosity and water absorption initially decrease but later increase as the ratio continues to rise. Lower water content leads to higher compressive strength and density, whereas higher water content reduces strength and density. However, porosity and water absorption increase with higher water content. These findings underscore the intricate interplay between the Si/Al and W/MK ratios, which significantly influence the mechanical and physical characteristics of geopolymer materials, highlighting the importance of optimizing these parameters for desired performance outcomes.

Acknowledgement

This scoping review was made possible by the support of the Iraq Ministry of Education and the

University of Technology in facilitating research related to sustainable materials.

Conflicts of Interest

The authors declare that there is no conflict of interest regarding the publication of this paper.

References

[1] Jindal, B. B., T. Alomayri, A. Hasan, and C. R. Kaze. 2022. Geopolymer Concrete with Metakaolin for Sustainability: A Comprehensive Review on Raw Materials' Properties, Synthesis, Performance, and Potential Application. *Environmental Science and Pollution Research.* 29: 1–26.

[2] Al-Shathr, B. S., T. S. Al-Attar, and Z. Hasan. 2015. Optimization of Geopolymer Concrete Based on Local Iraqi Metakaolin. In *Proceedings of the 2nd International Conference on Buildings, Construction and Environmental Engineering*. 97–100.

[3] Abbas, Z. K., A. A. Abbood, and R. S. Mahmood. 2022. Producing Low-Cost Self-Consolidating Concrete Using Sustainable Material. *Open Engineering*. 12: 850–58.

[4] Al Obeidy, N. F., W. I. Khalil, and H. K. Ahmed. 2024. Optimization of Local Modified Metakaolin-Based Geopolymer Concrete by Taguchi Method. *Open Engineering.* 14: 20220561.

[5] Alhifadhi, M. A., T. S. Al-Attar, and Q. A. Hasan. 2023. A Proposed New Mix Proportioning Method for Fly Ash-Based Geopolymer Concrete. *Engineering and Technology Journal.* 41: 1346–54.

[6] Al-Jabar, A., H. Al-Kaisy, and S. Ibrahim. 2022. Investigating the Effect of Different Parameters on Physical Properties of Metakaolin-Based Geopolymers. *Engineering and Technology Journal.* 40: 1–10. https://doi.org/10.30684/etj.2022.132691.1138.

[7] Albidah, A. S. 2021. Effect of Partial Replacement of Geopolymer Binder Materials on the Fresh and Mechanical Properties: A Review. *Ceramics International.* 47: 14923–43. https://doi.org/10.1016/j.ceramint.2021.02.127.

[8] Jha, V. K., and A. Tuladhar. 2011. An Attempt of Geopolymer Synthesis from Construction Waste. *Journal of Nepal Chemical Society* 28: 29–33.

[9] Jabar, T. A., M. A. Alzuhairi, and M. S. Abed. 2024. Acidic Influence on Geopolymerization: A Thorough Study Using HCl and Iraqi Kaolin. *Russian Journal of Applied Chemistry*. 97: 1–10.

[10] Jiang, T., Z. Liu, X. Tian, J. Wu, and L. Wang. 2024. Review on the Impact of Metakaolin-Based Geopolymer's Reaction Chemistry, Nanostructure, and Factors on Its Properties. *Construction and Building Materials.* 412: 134760. https://doi.org/10.1016/j.conbuildmat.2023.134760.

[11] Davidovits, J. 2013. Geopolymer Cement: A Review. *Geopolymer Institute Technical Papers.* 21: 1–11.

[12] Izquierdo, M., X. Querol, J. Davidovits, D. Antenucci, H. Nugteren, and C. Fernández-Pereira. 2009. Coal Fly Ash–Slag-Based Geopolymers: Microstructure and Metal Leaching. *Journal of Hazardous Materials.* 166: 561–66.

[13] Aliabdo, A. A., M. Abd Elmoaty, and M. A. Emam. 2019. Factors Affecting the Mechanical Properties of Alkali-Activated Ground Granulated Blast Furnace Slag Concrete. *Construction and Building Materials.* 197: 339–55.

[14] Al-Jabar, A., S. Ibrahim, and H. Al-Kaisy. 2021. Factors Affecting the Bond Strength of Geopolymer Repair Material: A Review. *Journal of Physics: Conference Series.* 1973: 012134. https://doi.org/10.1088/1742-6596/1973/1/012134.

[15] Kioupis, D., A. Skaropoulou, S. Tsivilis, and G. Kakali. 2022. Properties and Durability Performance of Lightweight Fly Ash–Based Geopolymer Composites Incorporating Expanded Polystyrene and Expanded Perlite. *Ceramics.* 5: 821–36.

[16] Yang, L., J. Zhang, C. Li, G. Wang, S. Duan, and K. Zhang. 2024. "Super Stable Coal Fly Ash–Based Solid Heat-Collecting Particles with Excellent Spectral Selectivity. *Solar Energy*. 276: 112666. https://doi.org/10.1016/j.solener.2024.112666.

[17] Khalil, W. I., W. A. Abbas, and I. F. Nasser. 2018. Some Properties and Microstructure of Fibre Reinforced Lightweight Geopolymer Concrete. In *Proceedings of the 2018 International Conference on Advance of Sustainable Engineering and Its Application (ICASEA)*. 147–52. https://doi.org/10.1109/ICASEA.2018.8370973

[18] Toniolo, N., A. Rincón, Y. S. Avadhut, M. Hartmann, E. Bernardo, and A. R. Boccaccini. 2018. Novel Geopolymers Incorporating Red Mud and Waste Glass Cullet. *Materials Letters.* 219: 152–54. https://doi.org/10.1016/j.matlet.2018.02.061.

[19] Jabar, T. A., A. Alzuhairi, and S. Abed. 2024. Utilizing Kaolin-Based Geopolymer Catalysts for Improved Doura Vacuum Residue. *Iraqi Journal of Oil & Gas Research.* 4.

[20] Park, S., and M. Pour-Ghaz. 2018. What Is the Role of Water in the Geopolymerization of Metakaolin? *Construction and Building Materials.* 182: 360–70.

[21] Al Obeidy, N. F., and I. Wasan. 2023. Studying the Possibility of Producing Paving Flags from Geopolymer Concrete Containing Local Wastes. *Engineering and Technology Journal.* 41: 1325–36.

[22] Mahdi, R. S., H. Dheaaldin, M. S. Abed, and A. B. Al-Zubaidi. 2023. Geopolymer Bricks from Iraqi Local Ores. In *AIP Conference Proceedings*. AIP Publishing.

[23] Oyebisi, S., F. Olutoge, P. Kathirvel, I. Oyaotuderekumor, D. Lawanson, J. Nwani, et al. 2022. Sustainability Assessment of Geopolymer Concrete Synthesized by Slag and Corncob Ash. *Case Studies in Construction Materials.* 17: e01665.

[24] Venkata Rao, M., R. Sivagamasundari, and T. Vamsi Nagaraju. 2023. Achieving Strength and Sustainability in Ternary Blended Concrete: Leveraging Industrial and Agricultural By-Products with Controlled Nano-SiO_2 Content. *Cleaner Materials.* 9: 100198. https://doi.org/10.1016/j.clema.2023.100198.

[25] Zhang, M., N. A. Deskins, G. Zhang, R. T. Cygan, and M. Tao. 2018. Modeling the Polymerization Process for Geopolymer Synthesis through Reactive Molecular Dynamics Simulations. *Journal of Physical Chemistry C*. 122: 6760–73.

[26] Chen, C.-C., Y.-K. Tsai, Y.-K. Lin, P.-H. Ho, and C.-Y. Kuo. 2023. Experimental and Numerical Investigation of the Mechanical Properties of a Fiber-Reinforced Geopolymer Mortar Blast-Resistant Panel. *Polymers.* 15: 3440.

[27] Hou, L., J. Li, and Z.-Y. Lu. 2019. Effect of Na/Al on Formation, Structures, and Properties of Metakaolin-Based Na-Geopolymer. *Construction and Building Materials.* 226: 250–58. https://doi.org/10.1016/j.conbuildmat.2019.07.171.

[28] Longhi, M. A., E. D. Rodríguez, B. Walkley, Z. Zhang, and A. P. Kirchheim. 2020. Metakaolin-Based Geopolymers: Relation between Formulation, Physicochemical Properties, and Efflorescence Formation. *Composites Part B: Engineering.* 182: 107671. https://doi.org/10.1016/j.compositesb.2019.107671.

[29] Al-Dujaili, M. A. A., I. A. D. Al-Hydary, and Z. Z. Hassan. 2021. Physical Characteristics and Compressive Strength of Na-Geopolymer Paste Designed by a Taguchi Method. *IOP Conference Series: Earth and Environmental Science*. 012036. IOP Publishing.

[30] Al-Sultani, S., I. Al-Hydary, and M. Al-Dujaili. 2021. Taguchi–Grey Relational Analysis for Optimizing the Compressive

Strength and Porosity of Metakaolin-Based Geopolymer. *International Journal of Engineering.* 34: 2525–33.

[31] Radhi, M. S., I. A. D. Al-Hydary, and A. M. H. Al-Ghaban. 2021. WITHDRAWN: Optimization of the Processing Parameters and Characterization of Hybrid Geopolymer Foam. *Materials Today: Proceedings*. https://doi.org/10.1016/j.matpr.2021.06.003.

[32] Alghannam, M., A. Albidah, H. Abbas, and Y. Al-Salloum. 2021. Influence of Critical Parameters of Mix Proportions on Properties of MK-Based Geopolymer Concrete. *Arabian Journal for Science and Engineering.* 46: 4399–4408.

[33] Huseien, G. F., M. Ismail, N. H. A. Khalid, M. W. Hussin, and J. Mirza. 2018. Compressive Strength and Microstructure of Assorted Wastes Incorporated Geopolymer Mortars: Effect of Solution Molarity. *Alexandria Engineering Journal.* 57: 3375–86.

[34] Rashad, A. M. 2013. Metakaolin as Cementitious Material: History, Sources, Production, and Composition—A Comprehensive Overview. *Construction and Building Materials.* 41: 303–18. https://doi.org/10.1016/j.conbuildmat.2012.12.001.

[35] Wan, Q., F. Rao, and S. Song. 2017. Reexamining Calcination of Kaolinite for the Synthesis of Metakaolin Geopolymers: Roles of Dehydroxylation and Recrystallization. *Journal of Non-Crystalline Solids.* 460: 74–80. https://doi.org/10.1016/j.jnoncrysol.2017.01.024.

[36] Mineralogical Society of Great Britain and Ireland. 1974. *The Infrared Spectra of Minerals*. London.

[37] Criado, M., A. Fernández-Jiménez, and A. Palomo. 2007. Alkali Activation of Fly Ash: Effect of the SiO_2/Na_2O Ratio. Part I: FTIR Study. *Microporous and Mesoporous Materials.* 106: 180–91. https://doi.org/10.1016/j.micromeso.2007.02.055.

[38] Shilar, F. A., S. V. Ganachari, V. B. Patil, T. Y. Khan, and S. D. A. Khadar. 2022. Molarity Activity Effect on Mechanical and Microstructure Properties of Geopolymer Concrete: A Review. *Case Studies in Construction Materials.* 16: e01014.

[39] Xie, J., and O. Kayali. 2014. Effect of Initial Water Content and Curing Moisture Conditions on the Development of Fly Ash-Based Geopolymers in Heat and Ambient Temperature. *Construction and Building Materials.* 67: 20–28.

[40] ASTM International. 2020. *ASTM C773-88a: Standard Test Method for Compressive (Crushing) Strength of Fired Whiteware Materials*. West Conshohocken, PA.

[41] ASTM International. 2006. *ASTM C373-88: Standard Test Method for Water Absorption, Bulk Density, Apparent Porosity, and Apparent Specific Gravity of Fired Whiteware Products*. West Conshohocken, PA.

[42] Kaya, M. 2022. The Effect of Micro-SiO_2 and Micro-Al_2O_3 Additives on the Strength Properties of Ceramic Powder–Based Geopolymer Pastes. *Journal of Material Cycles and Waste Management.* 24: 333–50. https://doi.org/10.1007/s10163-021-01323-3.

[43] Kim, B., and S. Lee. 2020. Review on Characteristics of Metakaolin-Based Geopolymer and Fast Setting. *Journal of the Korean Ceramic Society.* 57: 368–77. https://doi.org/10.1007/s43207-020-00043-y.

[44] Lizcano, M., H. Kim, S. Basu, and M. Radovic. 2012. Mechanical Properties of Sodium- and Potassium-Activated Metakaolin-Based Geopolymers. *Journal of Materials Science.* 47: 2607–16. https://doi.org/10.1007/s10853-011-6085-4.

[45] Duxson, P., J. L. Provis, G. C. Lukey, S. W. Mallicoat, W. M. Kriven, and J. S. J. van Deventer. 2005. Understanding the Relationship between Geopolymer Composition, Microstructure, and Mechanical Properties. *Colloids and Surfaces A: Physicochemical and Engineering Aspects.* 269: 47–58. https://doi.org/10.1016/j.colsurfa.2005.06.060.

[46] Duxson, P., G. Lukey, F. Separovic, and J. van Deventer. 2005. Effect of Alkali Cations on Aluminum Incorporation in Geopolymeric Gels. *Industrial & Engineering Chemistry Research.* 44: 832–39.

[47] Rees, C., G. Lukey, and J. van Deventer. n.d. The Role of Solid Silicates on the Formation of Geopolymers Derived from Coal Ash. Paper presented at the *International Symposium of Research Students on Material Science and Engineering*, Chennai, India.

[48] Mustofa, M., and S. Pintowantoro. 2017. The Effect of Si/Al Ratio on Compressive Strength and Water Absorption of Ferronickel Slag–Based Geopolymer. *IPTEK Journal of Proceedings Series.* 3: 167–72.

[49] Wei, X., F. Ming, D. Li, L. Chen, and Y. Liu. 2019. Influence of Water Content on Mechanical Strength and Microstructure of Alkali-Activated Fly Ash/GGBFS Mortars Cured at Cold and Polar Regions. *Materials.* 13: 138.

[50] Alshaaer, M., B. El-Eswed, R. Yousef, F. Khalili, and H. Rahier. 2016. Development of Functional Geopolymers for Water Purification and Construction Purposes. *Journal of Saudi Chemical Society.* 20 (Suppl.): S85–S92.

[51] Zhang, Z., and H. Wang. 2016. The Pore Characteristics of Geopolymer Foam Concrete and Their Impact on the Compressive Strength and Modulus. *Frontiers in Materials.* 3: 38.